

Statistical analysis of galaxy surveys - III: The non-linear clustering of red and blue galaxies in the 2dFGRS

Darren J. Croton¹, Peder Norberg², Enrique Gaztañaga³, Carlton M. Baugh⁴

¹*Department of Astronomy, University of California, Berkeley, CA, 94720, USA.*

²*SUPA*, Institute for Astronomy, University of Edinburgh, Royal Observatory, Blackford Hill, Edinburgh, EH9 3HJ, UK.*

³*Instituto de Ciencias del Espacio (IEEC/CSIC), F. de Ciencias UAB, Torre C5- Par-2a, Bellaterra, 08193 Barcelona, Spain.*

⁴*Institute for Computational Cosmology, Department of Physics, University of Durham, South Road, Durham DH1 3LE, UK.*

Accepted —. Received —; in original form —

ABSTRACT

We present measurements of the higher-order clustering of red and blue galaxies as a function of scale and luminosity made from the two-degree field galaxy redshift survey (2dFGRS). We use a counts-in-cells analysis to estimate the volume averaged correlation functions, $\bar{\xi}_p$, as a function of scale up to order $p = 5$, and also the reduced void probability function. Hierarchical amplitudes are constructed using the estimates of the correlation functions: $S_p = \bar{\xi}_p / \bar{\xi}_2^{p-1}$. We find that: 1) Red galaxies display stronger clustering than blue galaxies at all orders measured. 2) Red galaxies show values of S_p that are strongly dependent on luminosity, whereas blue galaxies show no segregation in S_p within the errors; this is remarkable given the segregation in the variance. 3) The linear relative bias shows the opposite trend to the hierarchical amplitudes, with little segregation for the red sequence and some segregation for the blue. 4) Faint red galaxies deviate significantly from the “universal” negative binomial reduced void probabilities followed by all other galaxy populations. Our results show that the characteristic colour of a galaxy population reveals a unique signature in its spatial distribution. Such signatures will hopefully further elucidate the physics responsible for shaping the cosmological evolution of galaxies.

Key words: galaxies: statistics, cosmology: theory, large-scale structure.

1 INTRODUCTION

The study of the large scale structure of the Universe is now entering a new phase. The two-degree field galaxy redshift survey (hereafter 2dFGRS; Colless et al. 2001, 2003) and the Sloan Digital Sky Survey (SDSS; York et al. 2000; Adelman-McCarthy et al. 2006) have yielded high precision measurements of the power spectrum of galaxy clustering on large scales (Cole et al. 2005; Tegmark et al. 2006; Percival et al. 2007; Padmanabhan et al. 2007). When these measurements are combined with high angular resolution maps of the temperature fluctuations in the cosmic microwave background radiation (e.g. Hinshaw et al. 2003, 2007), tight constraints can be derived on many of the parameters in the cold dark matter model (e.g. Sanchez et al. 2006; Spergel et al. 2007). Within this context, the emphasis in large scale structure studies is shifting to measuring the clustering signal for samples of galaxies defined by intrinsic properties such as luminosity, colour, morphology or spectral type, with the goal of developing our understanding of the physics of galaxy formation. The SDSS and 2dFGRS catalogues contain sufficiently

large numbers of galaxies over a large enough volume to allow robust measurements of clustering to be made for such subsamples (e.g. Norberg et al. 2001, 2002a; Zehavi et al. 2002, 2004, 2005; Madgwick et al. 2003).

There are many observational clues which point to a dependence of galaxy properties on their local environment. Dressler (1980) argued that galaxies follow a morphology-density relation, with the fraction of early-type galaxies increasing with the local density. Galaxy clusters have well defined red sequences in the colour-magnitude relation (Bower, Lucey & Ellis 1992; Stanford, Eisenhardt & Dickinson 1998). Analyses of the 2dFGRS and SDSS data sets have probed the connection between density and galaxy colour or type over a wider range of environments than was previously possible to reveal a general bimodality in the galaxy population (e.g. Lewis et al. 2002; Hogg et al. 2003, 2004; Balogh et al. 2004). These results suggest a tight correlation between the nature of a galaxy and its local environment, or equivalently the mass of its host dark matter halo. Measures of the clustering amplitude of different populations of galaxies reveal different results, indicating that these populations sample the underlying mass distribution in different ways. Hence, such clustering measurements can potentially tell us how

* The Scottish Universities Physics Alliance

the efficiency of the galaxy formation process depends upon halo mass.

The 2dFGRS and SDSS allow us to push measurements of galaxy clustering beyond the traditional two-point correlation function or power spectrum. By extending the clustering analysis to higher orders, we can extract new information about the connection between galaxies and matter. In previous work, we employed a counts-in-cells analysis to measure the higher-order correlation functions (Baugh et al. 2004; Croton et al. 2004b) and the void probability function (Croton et al. 2004a) for galaxies samples of different luminosity extracted from the 2dFGRS. We found that the higher-order correlation functions measured for 2dFGRS galaxies follow a hierarchical scaling pattern, characteristic of the clustering pattern which results from the growth of initially Gaussian fluctuations due to gravitational instability. Croton et al. (2004a) obtained independent confirmation of this result when they uncovered an unambiguous universal form for the void probability function. The values of the correlation functions do, however, show differences from the expectation for the best fitting cold dark matter model. Gaztañaga et al. (2005) measured the three-point correlation function without averaging over a cell volume, using triangles of galaxies with sides of varying length ratios. They found the first clear evidence for a non-zero second order or nonlinear bias parameter, suggesting that the relation of galaxies to the underlying dark matter may be more complicated than previous analyses had suggested (e.g. Verde et al. 2002; Lahav et al. 2002). Measuring the higher-order correlation functions is a challenging task, even with surveys of the size of the 2dFGRS and the SDSS. Baugh et al. (2004) found that their measurements of the correlation function for L^* galaxies in the 2dFGRS were affected on large scales by the presence of associations of rich clusters; Nichol et al. (2006) found similar effects in the SDSS.

In this paper, we extend our earlier work by exploiting the availability of colour information for the 2dFGRS catalogue. In Section 2 we briefly describe the 2dFGRS galaxy catalogue, the counts-in-cells approach we use and the statistics we measure, along with a reprise of how higher-order clustering measurements can be used to make deductions about galaxy bias. In Section 3 we present our results for the higher-order clustering of 2dFGRS galaxies selected by both luminosity and colour. We give a simple interpretation of these results in Section 4 and present a summary in Section 5.

2 DATA AND ANALYSIS

The methodology we use is identical to that described by Baugh et al. (2004) and Croton et al. (2004a; 2004b). These authors measured the higher-order clustering and the void probability function for galaxies as a function of luminosity, analysing volume limited samples drawn from the 2dFGRS. In this paper we extend this earlier work to consider samples defined by galaxy colour in addition to luminosity, as we did for the case of the 3-point correlation function in Gaztañaga et al. (2005). Full details of the clustering measurements and a complete discussion of their interpretation can be found in the above references; in this section, for completeness, we provide a brief outline of the 2dFGRS (§ 2.1), the statistics

measured (§ 2.2 and § 2.3) and give a recap of the implications of the higher-order clustering statistics for galaxy bias (§ 2.4).

2.1 The 2dFGRS galaxy catalogue

Our analysis employs the completed 2dFGRS (Colless et al. 2001; 2003) which contains a total of 221,414 unique, high quality galaxy redshifts down to a nominal magnitude limit of $b_J \approx 19.45$ with a median redshift $z \approx 0.11$. In addition to b_J -band magnitudes, R_F -band images have now been scanned, allowing a $b_J - R_F$ colour to be defined for each galaxy. To maximise the volume sampled, we restrict ourselves to regions with spectroscopic completeness in excess of 50%; however, in practice, the typical completeness is much higher than this in the final 2dFGRS, with the mean completeness in spheres of radius $< 10h^{-1}\text{Mpc}$ better than $\sim 80\%$. The remaining incompleteness is accounted for using the volume weighting corrections described in Croton et al. (2004b).

In order to construct a volume limited subsample from a flux limited redshift survey, it is necessary to model the redshift dependence of a galaxy’s luminosity or magnitude in the passband in which the survey selection is defined. We apply the colour dependent $k + e$ -correction model of Cole et al. (2005) to account for the average change in galaxy magnitude due to redshifting of the b_J -filter bandpass (the “ k -correction”) and also the associated typical galaxy evolution (the “ e -correction”). The purpose of defining a volume limited sample is to isolate galaxies of similar intrinsic luminosity in a sample with a simple radial selection function to facilitate clustering measurements (see Norberg et al. 2001; 2002a). Once such a sample has been constructed, we can subdivide it by galaxy colour, using the b_J and R_F -band photometry available for 2dFGRS data. Cole et al. (2005) analysed the rest frame $b_J - R_F$ colour distribution of galaxies in the 2dFGRS and found a clear division at a rest frame colour of $b_J - r_F = 1.07$. The bimodality in the colour distribution about this reference point leads to natural definition of “red” and “blue” galaxies. This separation by colour is similar, though by no means identical to the selection by spectral type employed in previous 2dFGRS analyses (Norberg et al. 2002a; Madgwick et al. 2002, 2003; Conway et al. 2005; Croton et al. 2005; see figure 2 of Wild et al. 2005).

The volume limited samples used in this paper are listed in Table 1 (see also table 1 of Croton et al. 2004b for further properties of these samples. Note that the improved $k + e$ -correction used here has resulted in small differences to the total number of galaxies falling within each volume limited boundary when compared with our previous work). Our analysis covers a wide range of luminosity, from $\sim 0.2L_{b_J}^*$ to $\sim 4L_{b_J}^*$ (the mean effective luminosities of the volume limited samples differ by a factor of 6 from the faintest to brightest). The error bars plotted on our measurements in each of the figures are jackknife estimates derived by subdividing each sample into 20 areas on the sky. Our measurements are strongly correlated from bin to bin, so it is essential to take this into account when fitting models to the measurements. For the purpose of deriving confidence intervals on fitted parameters, we compute a full covariance matrix using the ensemble of mock 2dFGRS catalogues described by Norberg

et al. (2002b). See section 4 for further details on how errors from the mocks are used in our analysis.

2.2 The distribution of counts-in-cells and its moments

The clustering statistics we employ require an accurate measurement of the count probability distribution function (CPDF) for the red and blue galaxy populations in our volume limited samples. This is done using a counts-in-cells (CiC) analysis. The CPDF for a given smoothing scale is measured by throwing down a large number (2.5×10^7) of spheres of radius R within the survey volume. The probability of finding exactly N galaxies within a sphere of this scale is given by:

$$P_N(R) = \frac{N_N}{N_T}. \quad (1)$$

Here $P_N(R)$ is the CPDF at the given scale R , where N_N is the number of spheres containing N galaxies out of a total of N_T spheres used. From the CPDF, the clustering moments of the distribution can be calculated directly. For example, the volume-averaged 2-point correlation function is given by

$$\bar{\xi}_2(R) = \left[\sum_{N=0}^{\infty} P_N(R) (N/\bar{N} - 1)^2 \right] - 1/\bar{N}, \quad (2)$$

where the mean number of galaxies expected in the sphere, \bar{N} , is simply

$$\bar{N} = \sum_{N=0}^{\infty} N P_N(R). \quad (3)$$

Expressions for the higher-order moments in terms of the CPDF are given in Appendix A of Gaztañaga (1994).

In the hierarchical model of galaxy clustering, all higher-order correlations can be expressed in terms of the 2-point function, $\bar{\xi}_2$, and dimensionless scaling coefficients, S_p (see Bernardeau et al. 2002):

$$\bar{\xi}_p = S_p \bar{\xi}_2^{p-1}. \quad (4)$$

Traditionally, $S_3 = \bar{\xi}_3/\bar{\xi}_2^2$ is referred to as the *skewness* of the distribution and $S_4 = \bar{\xi}_4/\bar{\xi}_2^3$ as the *kurtosis*. Given that both $\bar{\xi}_2$ and $\bar{\xi}_p$ ($p > 2$) can be evaluated using the CPDF, the hierarchical amplitudes S_p can readily be measured and the scaling behaviour of Eq. 4 tested (i.e. the validity of the $p - 1$ power law dependence for higher-order correlations; see Baugh et al. 2004).

2.3 The void probability function

A complementary way in which to study the hierarchical clustering paradigm is through the reduced void probability function (VPF). Put simply, the reduced VPF, χ , is a parametrisation of P_0 , the probability of finding an empty sphere in the galaxy distribution, in terms of the expectation from a purely Poisson galaxy distribution:

$$\chi = -\ln(P_0) / \bar{N}. \quad (5)$$

White (1979) derived Eq. 5 after writing the void probability function as a power series expansion in the moments of the CPDF ($\bar{\xi}_p$) to all orders. Under the hierarchical ansatz of

Eq. 4, this expansion can be expressed as a function of $\bar{N}\bar{\xi}_2$ only:

$$\chi(\bar{N}\bar{\xi}_2) = \sum_{p=1}^{\infty} \frac{S_p}{p!} (-\bar{N}\bar{\xi}_2)^{p-1}. \quad (6)$$

Therefore, if the hierarchical assumption is valid, a plot of χ as a function of $\bar{N}\bar{\xi}_2$ should produce a universal curve for galaxy catalogues with different mean densities and clustering properties, assuming common hierarchical amplitudes for the different populations (we will test this assumption in Section 3.2). Note that clustered tracers which deviate strongly from a Poisson distribution will have VPF values $\chi < 1$.

The precise form of the reduced VPF is set by the hierarchical amplitudes, S_p , for which different models of clustering predict different values. Here we summarise only the most successful model, the *negative binomial model*, which does very well at reproducing the measurements from the 2dFGRS for both the VPF (Fig. 3 in Croton et al. 2004b) and the hierarchical amplitudes, S_p (Table 1 in Baugh et al. 2004). The reduced VPF and hierarchical amplitudes for the negative binomial model are

$$\begin{aligned} \chi &= \ln(1 + \bar{N}\bar{\xi}_2) / \bar{N}\bar{\xi}_2 \\ S_p &= (p - 1)! \end{aligned} \quad (7)$$

Further analytic models, like the minimal and thermodynamic, are explored in Croton et al. (2004b).

2.4 Higher-order moments and relative bias

The distribution of galaxies could be quite different from that of the underlying dark matter. One could conceive of physical processes which could lead to a dependence of the efficiency of galaxy formation on the mass and perhaps the environment of dark matter haloes (e.g. Croton, Gao & White 2007). If this is indeed the case, galaxies should be regarded as *biased* tracers of the matter distribution.

A simple model for galaxy bias was introduced by Fry & Gaztañaga (1993). These authors assumed that the density contrast in the galaxy distribution, δ^G , can be expressed as a general non-linear function of the density contrast of the dark matter, δ^{DM} , so that: $\delta^G = F[\delta^{\text{DM}}]$. For density fluctuations smoothed on large enough scales so that the matter density contrast is of the order unity or smaller, this relation can be expanded in a Taylor series:

$$\delta^G = \sum_{k=0}^{\infty} \frac{b_k}{k!} (\delta^{\text{DM}})^k. \quad (8)$$

On scales where the variance, $\bar{\xi}^{\text{DM}}$, is small, the leading order contribution to the variance is dominated by the linear term:

$$\bar{\xi}_2^G = b_1^2 \bar{\xi}_2^{\text{DM}} + O[\bar{\xi}_2^{\text{DM}}]^2, \quad (9)$$

where b_1 is the so-called ‘‘linear bias’’, b . The leading order term in the expansion for the skewness, S_3 , is:

$$S_3^G = \frac{1}{b_1} (S_3^{\text{DM}} + 3c_2), \quad (10)$$

where we use the notation $c_2 = b_2/b_1$ (expressions for the hierarchical amplitudes up to $p = 7$ are given in Fry &

Table 1. The basic properties of the galaxy samples used in this paper (columns 1-3) and the best fitting relative linear bias b_r (Eq. 11; column 4) and relative non-linear bias c'_2 (Eq. 13; column 5). Also shown are the best fitting S_p measurements to the hierarchical ratios plotted in Fig. 2 (columns 6-8). The three sections give the properties and results for red galaxies, blue galaxies, and all colours combined (included to facilitate comparison with earlier work). All errors correspond to the 95 % confidence interval (2-sigma) for fits carried out using measurements in the range $R = 4.5 - 14h^{-1}\text{Mpc}$.

population	Mag. range $M_{b_j} - 5 \log_{10} h$		N_{gal}	b_r (Eq. 11)	c'_2 (Eq. 13)	S_3	S_4	S_5
RED GALAXIES	-18.0	-19.0	7710	0.97 ± 0.06	0.25 ± 0.15	2.83 ± 0.37	13.5 ± 4.5	80 ± 50
	-19.0	-20.0	18693	0.89 ± 0.04	0.13 ± 0.16	2.69 ± 0.34	12.2 ± 4.3	74 ± 50
	-20.0	-21.0	15147	1	0	2.04 ± 0.15	6.4 ± 2.4	28 ± 15
BLUE GALAXIES	-18.0	-19.0	14086	0.84 ± 0.05	-0.11 ± 0.09	2.00 ± 0.13	5.35 ± 1.78	11.0 ± 6.5
	-19.0	-20.0	22499	0.90 ± 0.04	-0.06 ± 0.10	2.09 ± 0.14	6.66 ± 1.47	29 ± 23
	-20.0	-21.0	15125	1	0	1.83 ± 0.13	4.28 ± 0.94	10.0 ± 5.5
RED+BLUE GALAXIES	-18.0	-19.0	21796	0.85 ± 0.06	0.02 ± 0.12	2.44 ± 0.32	9.46 ± 3.15	46 ± 33
	-19.0	-20.0	41192	0.88 ± 0.04	0.00 ± 0.11	2.35 ± 0.30	8.77 ± 3.27	44 ± 36
	-20.0	-21.0	30272	1	0	2.01 ± 0.14	5.97 ± 1.31	24 ± 13

Gaztañaga 1993). S_3^{DM} encodes the non-linear gravitational evolution of the matter distribution from Gaussian initial conditions. Hence, two non-linear effects are present in S_3^{G} : gravity (i.e. as contained in S_3^{DM}) and galaxy bias (i.e. as quantified by c_2). Both terms are modulated by the linear bias, b_1 . Therefore, in general, the interpretation of the skewness measured in the galaxy distribution is not trivial. However, on weakly non-linear scales we have detailed models of what to expect for the skewness of the dark matter (see, for example, Bernardeau et al. 2002; calculations have also been carried out for non-standard gravitational models and cosmologies – see Gaztañaga & Lobo 2001). We can therefore hope to learn about non-linear galaxy biasing if we can measure the skewness in the galaxy distribution, S_3^{G} , on scales on which the underlying fluctuations are only weakly non-linear.

It is useful to define a *relative* bias to aid with the interpretation of measurements of higher-order clustering. The relative bias describes the change in clustering signal compared to that measured for a reference sample. Using Eq. 9 as a guide, we define the relative linear bias of a sample, $b_r = b_1/b_1^*$, as the square root of the ratio of the 2-point correlation function (or variance) measured for the sample, relative to that found for the reference sample, denoted by an asterisk:

$$b_r \equiv \frac{b_1}{b_1^*} = \left(\frac{\bar{\xi}_2^{\text{G}}}{\bar{\xi}_2^{\text{G}*}} \right)^{1/2}. \quad (11)$$

Our reference sample is the volume limited population of galaxies in the magnitude range $-20 > M_{b_j} - 5 \log_{10} h > -21$, which is one magnitude brighter than the one used in Croton et al. (2004a). The reason for choosing a brighter sample is directly related to the influence the large coherent superstructures have on the L^* sample: it makes more sense to use as reference a sample which is not systematically affected by the presence of such rare massive structure. For completeness, in Table 1 we show the relative bias results for the volume limited “all colour” catalogues analysed in Cro-

ton et al. (2004a), however now presented relative to this brighter reference sample.

On scales for which a linear bias is a good approximation, i.e. when $b_k \simeq 0$ for $k > 1$, we can relate the S_p^{G} measured for different galaxy samples regardless of the value of S_p^{DM} for the underlying mass:

$$S_p^{\text{G}} = \frac{S_p^{\text{G}*}}{b_r^{p-2}}. \quad (12)$$

More generally, if galaxy bias is non-linear one can introduce a measure to quantify the relative non-linear bias:

$$c'_2 = \frac{(c_2 - c_2^*)}{b_1^*} = \frac{1}{3} (b_r S_3^{\text{G}} - S_3^{\text{G}*}), \quad (13)$$

where an asterisk denotes a quantity measured for the reference sample. In general, if the reference sample is un-biased (i.e. $b_1^* = 1$ and $c_p^* = 0$), we then have $c'_2 = c_2$ and $b_r = b_1$ for all samples.

3 RESULTS

In this section we present the main results of the paper, which are inferred from our measurement of the count probability distribution function (CPDF), as outlined in Section 2, for the samples of red and blue galaxies listed in Table 1. We present the volume averaged correlation functions, $\bar{\xi}_p$, in § 3.1, the hierarchical amplitudes, S_p , in § 3.2, and the reduced void probability function (VPF) in § 3.3.

3.1 The higher-order correlation functions

Fig. 1 shows the volume averaged correlation functions for orders $p = 2-5$ as a function of smoothing scale. The left hand panel shows the measurements for red galaxies and the right panel for blue galaxies. In both panels the symbols show the results for samples in the magnitude range $-19 > M_{b_j} - 5 \log_{10} h > -20$ (i.e. approximately $L_{b_j}^*$), while the adjacent dashed and dotted lines show samples which are

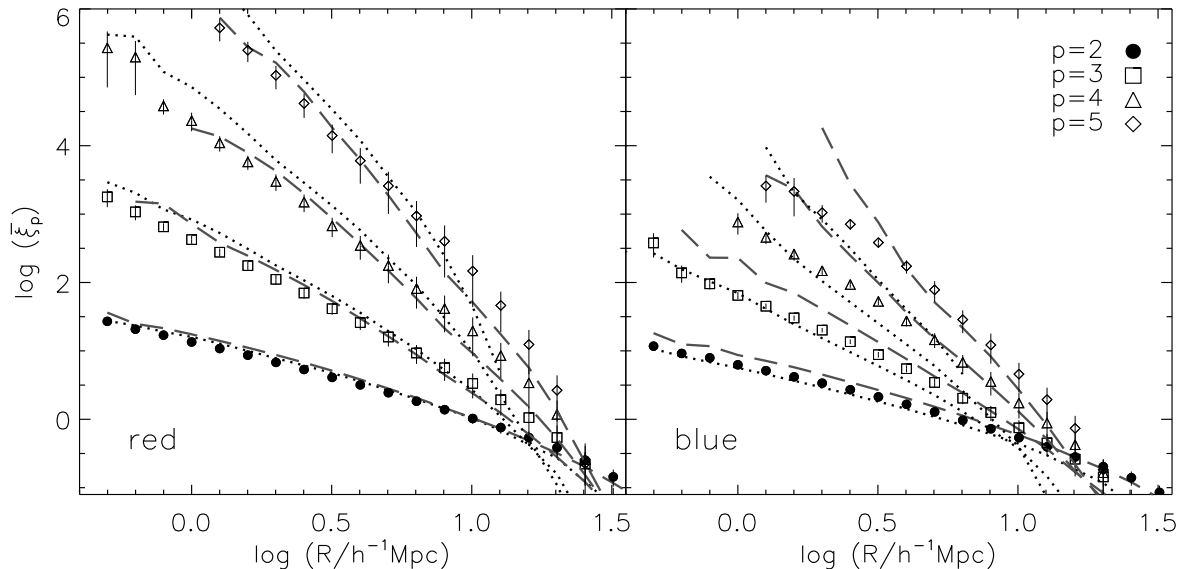


Figure 1. The p -point volume averaged correlation functions as a function of scale. The left and right panels show results for red and blue galaxies separately. In each panel, the symbols denote galaxies in the magnitude range $-19 > M_{b_j} - 5 \log_{10} h > -20$, while the adjacent dashed and dotted lines show the clustering measured for galaxies defined by magnitude ranges which are, respectively, one magnitude brighter and fainter (Table 1). Different symbols show different orders of clustering, as indicated by the key.

one magnitude brighter and fainter respectively. The order of volume averaged correlation function is indicated by the symbol type shown in the legend.

Red galaxies clearly show a larger clustering amplitude than the equivalent population of blue galaxies, as expected from earlier results obtained for the two-point correlation function as a function of colour (e.g. Zehavi et al. 2005 in the SDSS) or spectral type (Norberg et al. 2002a; Madgwick et al. 2003 in the 2dFGRS). The dependence of clustering strength on galaxy luminosity appears to be the strongest for the blue population, with the faintest blue galaxies being more weakly clustered than the brightest. The situation is more complicated for red galaxies; both the faintest and brightest samples of red galaxies appear to be more strongly clustered than the red L^* sample. There is even a suggestion that the faintest red galaxies become the more strongly clustered with increasing order, although the errors on the measurements are also increasing at a fixed scale for higher values of p . This type of behaviour was noted previously for the two-point correlation function. Norberg et al. (2002b) found an increase in the correlation length of early spectral types for samples faintwards of L^* , with the faintest early types displaying a similar correlation length to the brightest early types. Zehavi et al. (2005) found a similar increase in clustering strength for faint red galaxies. This trend can be readily explained; the satellite population in massive clusters is predominantly made up of faint, red galaxies and clusters are known to be strongly biased tracers of the mass distribution (e.g. Padilla et al. 2004).

3.2 The hierarchical amplitudes

Fig. 2 extends the results presented in the previous subsection by plotting the hierarchical amplitudes (as defined by

Eq. 4), S_3 (the skewness), S_4 (the kurtosis) and S_5 , as a function of scale. This is done for red galaxies in the left panel and blue galaxies in the right panel. Again, the results are shown for samples with different luminosities, with symbols representing the measurement of galaxies in the magnitude range $-19 > M_{b_j} - 5 \log_{10} h > -20$, and dashed and dotted lines showing the S_p for samples one magnitude brighter and fainter than this respectively. Red galaxies show a strong segregation of the hierarchical amplitudes with luminosity at a given clustering order; the S_p for blue galaxies show little dependence on luminosity.

On large scales, N-body simulations and perturbation theory suggest that the hierarchical amplitudes for the mass should only vary slowly with scale in the case of initially Gaussian fluctuations which grow through gravitational instability (e.g. Juskiwicz, Bouchet & Colombi 1993; Baugh et al. 1995; for a summary of the theoretical predictions, see Bernardeau et al. 2002). Observationally, the hierarchical amplitudes for galaxies have traditionally been measured to be either approximately constant or decreasing slowly out to progressively larger smoothing scales (e.g. Gaztañaga 1992; Bouchet et al. 1993; Gaztañaga 1994; Hoyle, Szapudi & Baugh 2000; Frith, Outram & Shanks 2006; see Bernardeau et al. 2002 for a review of previous measurements). However, recent work has shown that the presence of large, rare superstructures in the galaxy distribution can produce a significant upturn in the value of S_p on large scales (e.g. Szapudi & Gaztañaga 1998; Baugh et al. 2004; Croton et al. 2004b; Nichol et al. 2006). According to figure 10 from Gaztañaga et al. (2005), the upturn in the hierarchical amplitudes appears to be equally important when using measurements of the 3-point correlations function of red and blue galaxies from the 2dFGRS $-19 > M_{b_j} > -20$ sample. Nevertheless, it should be emphasised that, in the

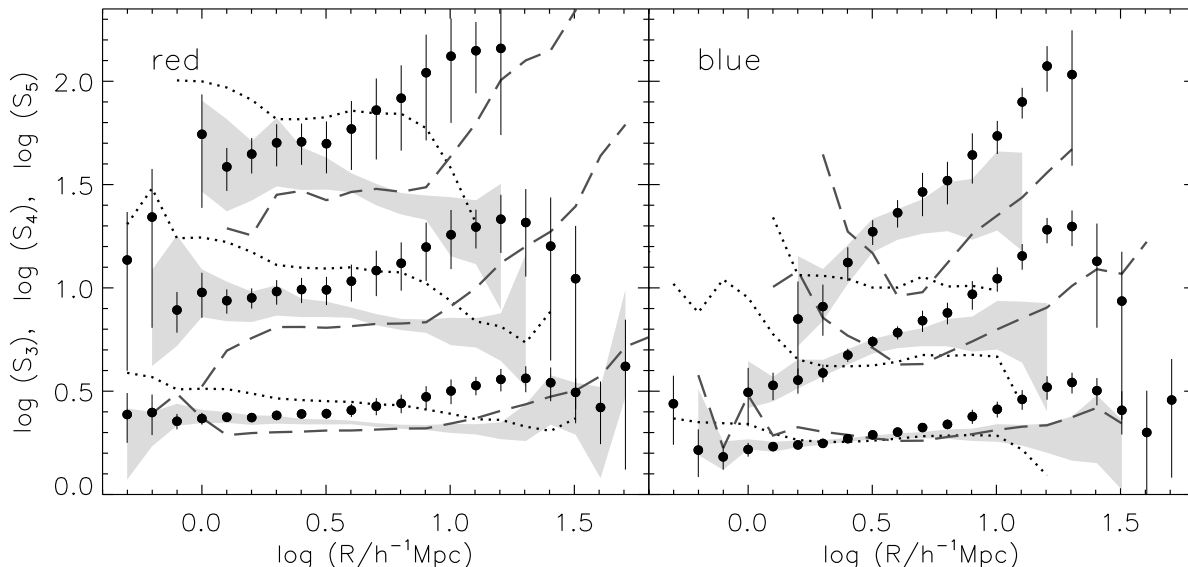


Figure 2. The hierarchical amplitudes, S_p , plotted as a function of scale. The left panel shows the results for red galaxies and the right panel those obtained for blue galaxies. The symbols and lines have the same meaning as those used in Fig. 1. The grey shaded regions show how the results for the $L_{b,J}^*$ galaxy sample change when the two largest superstructures are excluded from the CiC analysis, as described in the text.

case of the 2dFGRS, the impact of the superstructures on the measured hierarchical amplitudes is most pronounced in the $-19 > M_{b,J} - 5 \log_{10} h > -20$ volume limited sample and is essentially negligible in the brighter and fainter samples. This is due to the superstructures falling entirely within the redshift interval spanned by the L^* sample. In the case of the fainter volume limited sample, the superstructures lie mostly beyond the maximum redshift which defines the sample, whilst in the case of the brighter sample, the volume covered is much larger and the significance of the superstructures is correspondingly lower. See Croton et al. (2004b), Baugh et al. (2004) and Gaztañaga et al. (2005) for detailed investigations into how these two superstructures affect the measurement of higher-order statistics. The flatness of the earlier results for the S_p can be understood by noting that a) most smaller surveys never intersected with these rare superstructures of galaxies, b) their influence for larger surveys, such as the original 2dFGRS parent catalogue, the APM Survey (i.e. Gaztañaga 1994) or 2MASS (Frith, Outram & Shanks 2006), was diluted by the significant increase in sample volume, and c) typically any contribution from large coherent superstructures is downgraded in a flux limited catalogue rather than a volume limited sample due to the varying selection function.

In Fig. 2, the grey shaded regions show the results for the hierarchical amplitudes measured from the $L_{b,J}^*$ sample after removing the two large superstructures identified in Baugh et al. (2004). The shaded regions indicate the extent of the $1-\sigma$ errors on the measurements and should be compared with the symbols and error bars, which show the results for the same volume limited sample but *without* removing the superstructures from the CiC analysis. By omitting the two superstructures, the theoretically expected constant behaviour of S_3 is restored for larger smoothing lengths.

However, whilst the results change on large scales for S_4 and S_5 on removing the superstructures, there is still significant scale dependence of the S_p with opposite gradients found for red and blue galaxies. From Fig. 2, the impression is that the red population is the most strongly affected by the presence of the superstructures¹. This behaviour should be contrasted with the measurements by Croton et al. (2004b) and Baugh et al. (2004) made using the full $L_{b,J}^*$ sample. In these papers, removing the superstructures from the CiC analysis, led, to within the accuracy of the measurements, to all the hierarchical moments up to 5th order becoming roughly independent of scale. Our results for red and blue galaxies imply that the L^* results for all galaxies were due to a fortuitous cancellation of the trends with scale seen for red and blue galaxies.

Finally, it is worth noting that the upturn seen on small scales in both S_4 and S_5 for the bright and faint populations of blue galaxies is not statistically significant: in both cases, the jackknife errors, if plotted, are fully consistent with no upturn at all.

3.3 The reduced void probability function

In Fig. 3 we plot the reduced void probability function (VPF) for the three luminosity samples (using different symbols as shown by the legend) and for red and blue galaxy populations (left and right hand panels respectively). Previous measurements have revealed that galaxy samples defined by luminosity (or equivalently number density) display a universal form for the VPF (e.g. Croton et al. 2004a;

¹ A robust quantitative statement would require the use of more realistic mocks, for which colour dependent absolute errors on S_p can be derived.

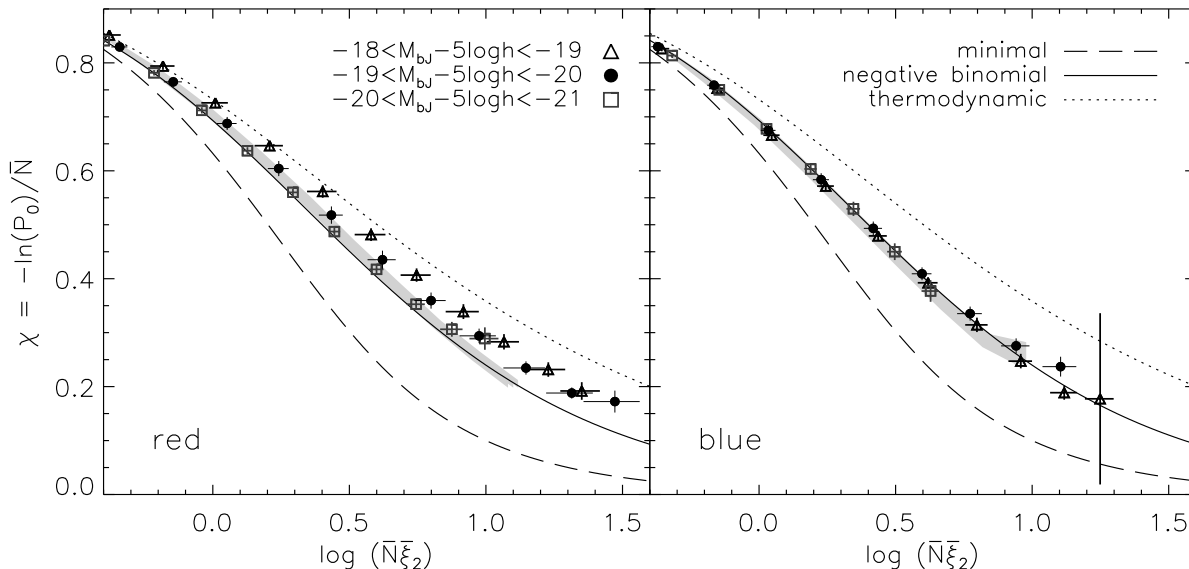


Figure 3. The reduced void probability function plotted as a function of the scaling variable $\bar{N}\bar{\xi}$. Left and right panels show the measurements for the red and blue populations respectively, while the symbols denote galaxy samples of different luminosity as indicated by the legend. The grey shaded region shows how the results change for the L_{bj}^* sample when the two largest superstructures are removed from the analysis.

Hoyle & Vogeley 2004; Patiri et al. 2006). This universality also holds for samples at different redshifts (Conroy et al. 2005; 2007). The recovery of a universal form for the VPF is evidence for the hierarchical scaling of the higher-order correlation functions of galaxies (e.g. Eq 4). The actual form of the VPF curve is well described, in redshift space, by the negative binomial model (see also Fry 1986 and Gaztañaga & Yokoyama 1993).

Here we report a significant departure from the universal scaling of the VPF. As can be seen in Fig. 3, the VPF measured for *red* galaxies deviates from the universal scaling in a way such that the deviation is strongest for the faintest galaxies considered. The VPF measured for blue galaxies, on the other hand, shows no dependence on luminosity, and matches almost perfectly the negative binomial model across the entire range plotted. Note that the deviation seen for the red L_{bj}^* population appears to arise from the contribution of the two superstructures discussed in the previous subsection. Once these large structures are removed from the analysis and the VPF is recalculated, the results for the L_{bj}^* sample shift back to the negative binomial model, as shown by the grey shaded region. On the other hand, the fainter red galaxy sample (shown by the triangles in Fig. 3), which is not affected by the two superstructures, does not agree with the negative binomial model. This disagreement persists if we consider even fainter samples, which we have not plotted in the figure for clarity.

Our results show that once we have accounted for the difference in mean density and clustering, faint red galaxies have a characteristically larger VPF than is measured for the other galaxy samples. From Eq. 6, we expect that samples with a larger VPF should also have larger values for the S_p , and this is borne out by the results given in Table 1, which are discussed in the next section. A high value for S_p

indicates non-linear biasing. If one were to simply increase the *linear* bias, this would increase the amplitude of the correlation functions, $\bar{\xi}_p$, but would reduce the hierarchical amplitudes (see Eq. 4 and Eq. 12). A non-zero non-linear bias is characteristic of the high density regions of the dark matter distribution. This is in line with the suggestion made above that the red faint galaxies could be made up of a significant population of satellites in clusters.

The reasons behind the success of the negative binomial model for the VPF are unclear. Vogeley et al. (1994) showed that the VPF measured in their simulations only agreed with the negative binomial model when the clustering pattern was distorted by peculiar motions; the VPF measured in real space did not match the negative binomial model. However, our results imply that the peculiar motions of galaxies are not the primary agent responsible for the success of the negative binomial model. We find that the faint red galaxies, which are primarily satellites within galaxy clusters and hence likely to display large peculiar motions, in fact show the strongest departure from the VPF predicted by the negative binomial model, rather than being driven towards this model.

4 DISCUSSION

In this section we give some simple interpretations of the measurements of the hierarchical amplitudes reported in Section 3.2. This requires us to perform fits to the measurements, in the first case by extracting best fitting values for the hierarchical amplitudes, S_p (as defined in Eq. 4), and then to constrain the linear and non-linear bias parameters (see Eq. 11 and Eq. 13).

Measures of the hierarchical amplitudes on different

smoothing scales are correlated, a fact which has often been ignored in previous analyses reported in the literature. The existence of a bin-to-bin correlation is clearly demonstrated by the response of our estimates of the hierarchical amplitudes to the removal of the two largest superstructures in the 2dFGRS. Given this correlation, it is necessary to construct a covariance matrix for the measurements in order to carry out meaningful fits. One way to do this is to use a jackknife approach in which the survey volume is split into a number of equal sized subvolumes, on the order of 20 (if not more to construct a stable covariance matrix). Unfortunately, this is infeasible for our fainter volume limited samples, as the volume covered in these cases is too small to be subdivided an appropriate number of times. Instead, we use the ensemble of mock 2dFGRS catalogues whose construction is described in Norberg et al. (2002b). Particles were chosen from an N-body simulation to represent galaxies using a simple parametric function of the local smoothed density of dark matter (see Cole et al. 1998 for a description of the bias algorithm). The parameters in this empirical biasing prescription were constrained to reproduce the typical clustering measured in the full flux limited 2dFGRS (Hawkins et al. 2003). Consequently, one limitation of the mock catalogues is that the luminosity and colour assigned to a “galaxy” is independent of the local density of the particle. This means that the mocks do not display any dependence of clustering on luminosity or colour. Also, no information about the higher-order clustering of mock galaxies was used to select the parameters in the bias prescription. Hence, although the two point correlation function for mock galaxies agrees very closely with that measured for the full 2dFGRS, there is no guarantee that the higher-order clustering in the mocks will look like that measured in the real survey.

As we found in our earlier work using the mocks (Croton et al. 2004b; Gaztañaga et al. 2005), the covariance matrices estimated from the mocks are stable and give robust estimates of best fitting quantities and the associated errors. A principal component decomposition of the covariance matrix reveals that the first few eigenvectors are typically responsible for the bulk of the variance or signal. We rank the eigenvectors in order of decreasing variance and retain sufficient eigenvectors to account for, at least, 95% of the variance.

We first perform fits to extract values for the scale *independent* hierarchical amplitudes. Although our results may appear in some cases to show a strong dependence on cell radius (Fig. 2), it is important to bear in mind that we can only show the diagonal part of the covariance matrix in plots and our fitting procedure takes into account the covariance between bins. Moreover, since there is a tradition of fitting constants to estimates of the S_p over a range of scales, it is useful to repeat such an analysis for our measurements in order to facilitate comparisons with previous work. We restrict our attention to the S_p values obtained for spheres with radii in the range $R = 4.5 - 14h^{-1}$ Mpc. These are slightly larger scales than we used in Croton et al. (2004b), since we aim to avoid scales which may be affected by shot noise, and our samples, as a result of being split by colour, typically have half the number of galaxies in each luminosity bin than before. To help with a comparison to our earlier work we also re-analyse the “all colour” galaxy catalogues across this new fitting range (note that these galaxies also differ in their improved $k + e$ corrections, as described in Section 2.1). The

results of a one parameter fit (S_p) to the hierarchical amplitudes are quoted as a function of luminosity for all galaxy colours and also the red and blue populations separately in Table 1, in which we also give the 95 % confidence interval around the best fitting value.

Next we constrain the relative bias parameters defined in Eq. 11 and Eq. 13. Recall that in this paper we define our reference sample to be volume limited galaxies in the magnitude range $-20 > M_{b_j} - 5 \log_{10} h > -21$. The error in the relative linear bias is straightforward to find using the mocks and the results are given in Table 1. Obtaining a robust fit for the nonlinear bias, c_2 , is more subtle. By construction, the mocks will return a zero nonlinear bias², whereas the expectation value for 2dFGRS samples can be anything. Therefore, in order to get a reliable estimate of the error on the best fitting nonlinear bias using the mocks, we need to take an indirect approach. We fit instead the combination $b_r S_3^G$, for which the mock catalogues are in rather good agreement with the real survey. Taking the best fitting value for the quantity $b_r S_3^G$, and the skewness measured for the reference sample, we can obtain a best fitting value for the nonlinear bias, c_2 , using Eq. 13. The error on the best fitting value is obtained by adding the errors on $b_r S_3^G$ and the skewness of the reference sample in quadrature, ie. assuming $b_r S_3^G$ and S_3^{G*} are uncorrelated. The resulting values of the nonlinear bias and the error on the best fit are listed in Table 1.

The results in Table 1 reveal substantial differences in the hierarchical amplitudes obtained for red and blue galaxies and in the way in which these amplitudes change with luminosity. Overall, we find that blue galaxies display smaller hierarchical amplitudes than red galaxies. Red galaxies show a significant change in S_p with luminosity, whereas blue galaxies show no such trend. Assuming Gaussian errors, we find a 3- σ shift in the best fitting S_3 between the faintest and brightest samples of red galaxies. In view of the relatively small baseline in luminosity over which we can perform such a fit, a factor of six in median luminosity moving from the faintest to the brightest volume limited sample, it is remarkable to see such a clear change in the higher-order clustering. These results are in good agreement with those found in Croton et al. (2004b) (see their Fig. 10). It is also noteworthy that the relative bias b_r quoted in Table 1, shows the opposite tendency to that displayed by the hierarchical amplitudes: there is little dependence of the linear relative bias on luminosity for red galaxies and a clear trend for blue galaxies.

Finally, it is encouraging to note that the conclusions we draw from our counts-in-cells analysis are consistent with those we reported in Gaztañaga et al. (2005, SAGS-II), who measured the 3-point correlation function for different triangle shapes and sizes (i.e. without averaging over the volume of a cell). In particular Fig. 7 in SAGS-II shows how for both equilateral and elongated triangles, late galaxies show little luminosity segregation in Q_3 , while early galaxies show a strong segregation, with Q_3 increasing with decreasing luminosity (see also Nishimichi et al. 2007).

² Without luminosity segregation, the expectation value for the mocks is $c_2 \approx 0$.

5 SUMMARY

This paper complements and extends previous clustering analyses of the 2dFGRS, taking advantage of the availability of R_F -band photometry to study the spatial distribution of galaxies as a function of *both* their colour and luminosity. We use a counts-in-cells approach to estimate the count probability distribution function (CPDF) of red and blue galaxies in different luminosity bins, spanning a factor of six in luminosity around L^* . From the CPDF, we estimate the volume-averaged higher-order correlation functions, $\bar{\xi}_p$, the hierarchical amplitudes, S_p , and the reduced void probability function for our galaxy samples, χ . We use our measurements of the hierarchical amplitudes to constrain the linear and nonlinear bias parameters in a simple model of galaxy clustering.

The main results of this paper can be summarised as follows:

- *Colour segregation in $\bar{\xi}_p$* : Blue galaxies show significantly lower clustering amplitudes than red galaxies. This trend holds up to the five point correlation function, extending the results previously reported for two-point correlations (e.g. Norberg et al. 2002a; Madgwick et al. 2003; Zehavi et al. 2005).

- *Luminosity segregation in $\bar{\xi}_p$* : Blue galaxies display a monotonic increase of clustering strength with luminosity, mirroring the results found for the two-point function of 2dFGRS galaxies (Norberg et al. 2002a). The behaviour of the red population is more complicated. Faint and bright red galaxies are more clustered than L^* red galaxies. A hint of this behaviour was previously found for the two-point correlation function of early spectral types in the 2dFGRS (which loosely correspond to the red sample in this paper) by Norberg et al. (2002a).

- *Luminosity segregation in S_p* : We fit scale-independent models to the hierarchical amplitudes which take into account the full covariance between adjacent bins. From this we conclude that the hierarchical amplitudes of blue galaxies show little or no dependence on galaxy luminosity. On the other hand, the hierarchical amplitudes of red galaxies vary strongly with luminosity. These new results, split by colour, explain why Croton et al. (2004b) found only a weak dependence of the S_p on luminosity.

- *Superstructures in the 2dFGRS*. The hierarchical amplitudes for the red galaxies seems to be more affected by the presence of the superstructures. After removing them, there is still significant scale dependence of the S_p , with opposite gradients found for red and blue galaxies. These results imply that the flatness of the L^* S_p measurements of Croton et al. (2004b) and Baugh et al. (2004), after removing the superstructures, are due to a fortuitous cancellation of the different trends with scale for red and blue galaxies.

- *The reduced void probability function*. Croton et al. (2004a) found that the reduced void probability function measured for 2dFGRS samples defined by luminosity displayed a universal form, and matches the one predicted by a negative binomial distribution. Splitting the samples by colour, we find that blue galaxies show the universal reduced void probability function consistent with the negative binomial, but red galaxies do not. The deviation from the negative binomial model is largest for faint red galaxies. This result is seemingly at odds with previous interpretations of

the success of the negative binomial model, in which it was suggested that galaxy peculiar motions were the primary agent behind the form of the reduced void probability function.

- *Linear and non-linear bias*. Fry & Gaztañaga (1993) introduced a simple model of galaxy bias in which the density contrast in galaxies is written as a Taylor expansion of the density contrast in the underlying mass. The first order bias term in this expansion is the common linear bias and the second order term is called the quadratic or nonlinear bias. We use our measurements of the variance and the skewness (S_p) to extract the linear and nonlinear bias parameters relative to the clustering in a reference sample. The reference sample is the one for which we are able to make our best measurements of galaxy clustering. In this paper, galaxies with magnitudes in the range $-21 < M_{b_J} - 5 \log_{10} h < -20$ are treated as the reference sample; there is a reference sample for red galaxies and one for blue galaxies. The relative bias parameters extracted for red and blue galaxies are different. The faintest red galaxies we consider have a linear bias consistent with that of the reference sample; red L^* galaxies have a linear bias below unity. For blue galaxies, the linear bias increases with luminosity. The relative non-linear bias for red galaxies is positive whereas that extracted for blue galaxies is negative. In all cases, these offsets are significant at the $1 - 2\sigma$ level.

Our measurements of the higher-order clustering of galaxies as a function of colour and luminosity provide valuable new constraints on models of galaxy formation. While the colour of a galaxy is determined by its star formation history, the clustering of galaxies, at least on the scales probed in this paper, is driven primarily by the mass of the host dark matter halo and to a lesser extent by the formation history of the halo (Gao et al. 2005; Harker et al. 2006; Wechsler et al. 2006; Croton, Gao & White 2007). Semi-analytical models of galaxy formation make *ab initio* predictions for the star formation histories of galaxies in a cosmological setting (see the review by Baugh 2006). This is done through simple physical prescriptions that describe those aspects of galaxy evolution believed to be important, including the rate of gas cooling, the timescale for star formation in galactic disks, mergers between galaxies, and feedback processes such as heating by supernova explosions or the accretion of material onto supermassive black holes. These processes are poorly understood and consequently, there is no unique way in which to model them.

At present there are a number of galaxy formation models which follow the evolution of disks and spheroids from high redshift to the present day (e.g. Baugh et al. 2005; Croton et al. 2006; Bower et al. 2006; Cattaneo et al. 2006; De Lucia & Blaizot 2007). The parameters that constrain the simple physics assumed in these models are typically set without reference to galaxy clustering. Higher-order clustering and non-linear bias measures are sensitive to how galaxies populate groups and clusters, and their periphery. We therefore look towards such statistics to further constrain and discriminate between different possible (and plausible) implementations of the galaxy formation physics. The higher-order spatial distribution of galaxies provides an additional window through which we can hope to understand the complex physics governing galaxy evolution.

ACKNOWLEDGEMENTS

The 2dFGRS was undertaken using the two-degree field spectrograph on the Anglo-Australian Telescope. We acknowledge the efforts of all those responsible for the smooth running of this facility during the course of the survey, the 2dFGRS team for carrying out the observations and releasing the data and also the support of the time allocation committees during the project. This work was supported in part by NSF grants AST00-71048 and AST05-07428, the Royal Society through the award of a Joint Project Grant, and by the European Commission through the ALFA-II programme's funding of the Latin American European Network for Astrophysics and Cosmology (LENAC). DC is supported by a DEEP2 postdoctoral fellowship. PN acknowledges receipt of a PPARC PDRA fellowship held at the IfA. EG acknowledges the Spanish Ministerio de Ciencia y Tecnologia (MEC), project AYA2006-06341 with EC-FEDER funding, research project 2005SGR00728 from Generalitat de Catalunya, the Galileo Galilei Institute for Theoretical Physics for hospitality, and the INFN for partial support during the completion of this work. CMB is funded by a Royal Society University Research Fellowship.

REFERENCES

- Adelman-McCarthy J.K., 2006, *ApJS*, 162, 38
 Balogh M., et al., 2004, *MNRAS*, 348, 1355
 Baugh C.M., Gaztañaga E., Efstathiou, G., 1995, *MNRAS*, 274, 1049
 Baugh C.M., et al., 2004, *MNRAS*, 351, L44
 Baugh C.M., et al., 2005, *MNRAS*, 356, 1191
 Baugh, C. M. 2006, *Reports of Progress in Physics*, 69, 3101
 Bernardeau F., Colombi S., Gaztañaga E., Scoccimarro R., 2002, *Phys. Rep.*, 367, 1
 Bouchet F.R., Strauss M.A., Davis M., Fisher K.B., Yahil A., Huchra J.P., 1993, *ApJ*, 417, 36
 Bower R.G., Lucey J.R., Ellis, R.S., 1992, *MNRAS*, 254, 601
 Bower, R. G., Benson, A. J., Malbon, R., Helly, J. C., Frenk, C. S., Baugh, C. M., Cole, S., & Lacey, C. G. 2006, *MNRAS*, 370, 645
 Cattaneo A., Dekel A., Devriendt J., Guiderdoni B., Blaizot J., 2006, *MNRAS*, 370, 1651
 Cole S., Hatton S., Weinberg D.H., Frenk C.S., 1998, *MNRAS*, 300, 656
 Cole S., et al., 2005, *MNRAS*, 362, 505
 Colless M.M., et al., 2001, *MNRAS*, 328, 1039
 Colless M.M., et al., 2003, *astro-ph/0306581*
 Conroy C., et al., 2005, *ApJ* 635, 990
 Conroy, C., et al. 2007, *ApJ*, 654, 153
 Conway E., et al., 2005, *MNRAS*, 356, 456
 Croton D.J., et al., 2004a, *MNRAS* 352, 828
 Croton D.J., et al., 2004b, *MNRAS* 352, 1232
 Croton, D. J., et al. 2005, *MNRAS*, 356, 1155
 Croton D.J., et al., 2006, *MNRAS* 365, 11
 Croton, D. J., Gao, L., & White, S. D. M. 2007, *MNRAS*, 374, 1303
 De Lucia, G., & Blaizot, J. 2007, *MNRAS*, 375, 2
 Dressler A., 1980, *ApJ*, 236, 351
 Frith, W. J., Outram, P. J., & Shanks, T. 2006, *MNRAS*, 373, 759
 Fry J.N., 1986, *ApJ*, 308, L71
 Fry J.N., Gaztañaga E., 1993, *ApJ*, 413, 447
 Gao, L., Springel, V., & White, S. D. M. 2005, *MNRAS*, 363, L66
 Gaztañaga E., 1992, *ApJ*, 398, L17
 Gaztañaga E., 1994, *MNRAS*, 268, 913
 Gaztañaga E., Yokoyama J., 1993, *ApJ*, 403, 450
 Gaztañaga E., Lobo J.A., 2001, *ApJ*, 548, 47
 Gaztañaga E., Norberg, P., Baugh, C. M., & Croton, D. J. 2005, *MNRAS*, 364, 620
 Harker G., Cole S., Helly J., Frenk C., Jenkins A., 2006, *MNRAS*, 367, 1039
 Hawkins E., et al., 2003, *MNRAS*, 346, 78
 Hinshaw G., et al., 2003, *ApJS*, 148, 119
 Hinshaw, G., et al. 2007, *ApJ*, 170, 288
 Hogg D.W., et al., 2003, *ApJ*, 585, L5
 Hogg D.W., et al., 2004, *ApJ*, 601, L29
 Hoyle F., & Vogeley M.S., 2004, *ApJ* 607, 751
 Hoyle F., Szapudi I., Baugh C.M., 2000, *MNRAS*, 317, L51
 Juszkiewicz R., Bouchet F.R., Colombi S., 1993, *ApJ*, 412, L9
 Lahav O., et al., 2002, *MNRAS*, 333, 961
 Lewis I., et al., 2002, *MNRAS*, 334, 673
 Madgwick D.S., et al., 2002, *MNRAS*, 333, 133
 Madgwick D.S., et al., 2003, *MNRAS*, 344, 847
 Nichol R.C., et al., 2006, *MNRAS*, 368, 1507
 Nishimichi, T., Kayo, I., Hikage, C., Yahata, K., Taruya, A., Jing, Y. P., Sheth, R. K., & Suto, Y. 2007, *PASJ*, 59, 93
 Norberg P., et al., 2001, *MNRAS*, 328, 64
 Norberg P., et al., 2002a, *MNRAS*, 332, 827
 Norberg P., et al., 2002b, *MNRAS*, 336, 907
 Padilla N.D., et al., 2004, *MNRAS*, 352, 211
 Padmanabhan, N., et al. 2007, *MNRAS*, 378, 852
 Patiri, S. G., Betancort-Rijo, J. E., Prada, F., Klypin, A., & Gottlöber, S. 2006, *MNRAS*, 369, 335
 Percival, W. J., et al. 2007, *ApJ*, 657, 645
 Sanchez A.G., Baugh C.M., Percival W.J., Peacock J.A., Padilla N.D., Cole S., Frenk C.S., Norberg P., 2006, *MNRAS*, 366, 189
 Spergel, D. N., et al. 2007, *ApJ*, 170, 377
 Stanford S.A., Eisenhardt P.R., Dickinson M., 1998, *ApJ*, 492, 461
 Szapudi I., Gaztañaga E., 1998, *MNRAS*, 300, 493
 Tegmark, M., et al. 2006, *PhRvD*, 74, 123507
 Verde L., et al., 2002, *MNRAS*, 335, 432
 Vogeley, M. S., Geller, M. J., Park, C., & Huchra, J. P. 1994, *AJ*, 108, 745
 Wechsler, R. H., Zentner, A. R., Bullock, J. S., Kravtsov, A. V., & Allgood, B. 2006, *ApJ*, 652, 71
 White S.D.M., 1979, *MNRAS* 186, 145
 Wild V., et al., 2005, 356, *MNRAS*, 247
 York D.G., et al., 2000, *AJ*, 120, 1579
 Zehavi, I., et al., 2002, *ApJ*, 571, 172
 Zehavi, I., et al., 2004, *ApJ*, 608, 16
 Zehavi, I., et al., 2005, *ApJ*, 630, 1